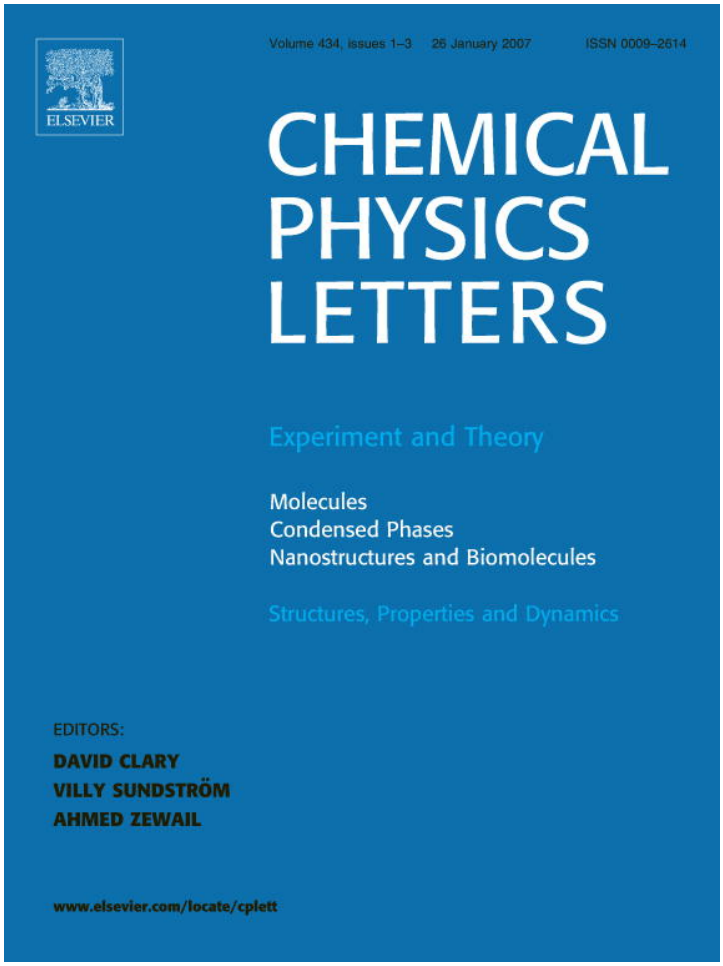

Available online at www.sciencedirect.com
ScienceDirect
Chemical Physics Letters 434 (2007) 78–81
CHEMICAL PHYSICS LETTERS
www.elsevier.com/locate/cplett

$FeCl_2$-CVD production of carbon fibres with graphene layers nearly perpendicular to axis

Thomas Laude *, Hiroaki Kuwahara, Kazuhiko Sato

Innovation Research Institute, Teijin Ltd, 2-1 Hinode-cho, Iwakuni, Yamaguchi 740-8511, Japan

Received 6 February 2006; in final form 22 November 2006
Available online 29 November 2006

Abstract

We decomposed acetylene by chemical vapour deposition in presence of $FeCl_2$ vapours, which react with carbon radicals without thermal decomposition (500 °C). This produced a large volume of wool-like product around the $FeCl_2$ reservoir, composed of semi-crystalline carbon fibres, with high conversion rate (40 mass%). Fibres showed remarkable morphology, with iron nano-rings belting their centres and mirror symmetry. Fibres were mono or multi filament (each filament belted with metal). Semi-crystalline fibres were readily transformed by thermal treatment into a large-angle conical structure with turbostratic piling along fibre axis. These observations suggest a catalytic growth on the inner wall of iron rings.

1. Introduction

Production of carbon fibres by chemical vapour deposition (CVD) of a carboneous compound (acetylene, benzene, CO, etc.) in presence of metallic catalyst nanoparticles is a method known since decades [1]. Fibres obtained by CVD are usually composed of concentric graphene cylinders parallel to axis, with micro or nano ('nanotubes') diameters. CVD catalyst particles can be supported on a substrate (silica, alumina, zeolites, etc.) [2], but substrate removal is cumbersome for large-scale production. Alternatively, catalyst particles can be produced by floating a gas/vapour catalyst precursor (ferrocene, iron-pentacarbonyl, etc.) to the reaction chamber. Catalyst particles are obtained by thermal decomposition of the metal precursor in gas phase [3].

CVD can also produce nano-fibres with layers oriented at various angles to fibre axis. Such fibres, with thickness 30–100 nm, were grown by decomposing several hydrocarbons over copper–nickel catalyst [4,5]. They sometime featured bi-directional growth (mirror symmetry at centre) with a metallic crystallite at fibre centre. Also, in recent years, plasma-enhanced CVD methods [6] have produced various types of nano-fibres with non-cylindrical structures, in particular 'bamboo' [7,8], and conical (or 'cup-stacked') [9–11] structures. Such thin nano-fibres with open edges on outer surface are interesting for their high surface area and functionalisation potential.

We have recently reported [12] that carbon nanotubes can be produced by CVD of acetylene in presence of floating $FeCl_2$. $FeCl_2$ reacts directly with carbon source without thermal decomposition. Hence, catalyst particle size and shape is not determined by the decomposition rate of the precursor as in usual floating CVD experiments.

Here, we report the growth of 100 nm to 1 μm thick carbon fibres with moustache-like morphology (we later call them 'Moustache fibres') having graphene layers roughly perpendicular to axis. We obtained those by changing growth conditions, and in particular by operating at low temperature (500 °C), well under $FeCl_2$ melting point (676 °C). As this fibre is suitable for large-scale production, low cost and readily crystallisable to turbostratic structure (hard carbon), it is of obvious interest for energy storage applications, and in particular for applications involving

* Corresponding author. Fax: +81 29 879 0051.
E-mail addresses: thomaslaude@uminokai.net, thomas.laude@airliquide.com (T. Laude).

0009-2614/$ - see front matter © 2006 Elsevier B.V. All rights reserved.
doi:10.1016/j.cplett.2006.11.091

the absorption of lithium or other chemical in the volume of the fibre.

2. Experimental

After leading many experiments with various experimental conditions, an efficient and reproducible experimental procedure was found as follows (see Fig. 1): A small ceramic boat ($30 \times 6 \times 3$ mm) was completely filled with 200 mg $FeCl_2$ anhydrous powder (Strem Chemicals 98%). The ceramic boat was capped by a quartz plate, maintained with two tightened aluminium strings. Two tungsten wedges were inserted on sides in order to have roughly a 0.1 mm opening between ceramic boat and quartz plate before reaction. This $FeCl_2$ reservoir was inserted in a short inner quartz tube (for easy collection), itself inserted in an atmosphere-controlled chamber (3 cm outer quartz tube) enclosed in a furnace ($FeCl_2$ reservoir at furnace centre, quartz plate below). The chamber was evacuated and maintained to primary vacuum for 30 minutes in presence of a cold trap (−80 °C). Argon (99.999%) was introduced in the chamber and flowed (500 ml/min, 10^5 Pa) during whole experiment except reaction time. After 30 min of argon flowing, temperature was risen from ambient to 500 °C (furnace thermocouple reading) in 15 min. Then, acetylene was flown (50 ml/min) for up to 40 min (reaction time). The chamber was cooled down (to 50 °C in 5 min) before opening.

An additional heat-treatment was undertaken at 2800 °C on 15 mg of raw wool-like product in a sealed-graphite-furnace under argon flow.

Transmission electron microscope (TEM) observations and electron diffraction analyses were performed with several Hitachi microscopes at 200, 300, and 800 kV, with thermal and field emission guns. For observation, the product was dispersed in ethanol by sonification and deposited on copper–carbon micro-grids. Electron diffractions could be performed locally on filaments thinner than 200 nm with the technique described previously [13]. Scanning electron microscope (SEM) observations were performed with several Hitachi microscopes at 3–25 kV, with thermal and field emission guns. The local elemental composition of fibres was analysed by energy dispersive X-ray (EDX) and calibrated with $FeCl_2$ powders. Thermo gravimetric analyses (TGA) were performed with Rigaku TG-8120 apparatus with 10 °C/min temperature rise and 100 ml/min airflow. Micro-Raman analyses were performed on a Jobin-Yvon T64000 at wavelength 514.5 nm. X-ray analyses were performed on a Rigaku wide-angle diffractometer using Cu Kα X-ray source.

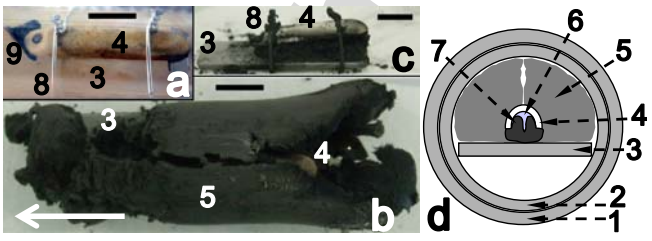

Fig. 1. Reactor around $FeCl_2$ reservoir: indexing 1, outer quartz tube; 2, inner quartz tube (short); 3, quartz plate; 4, ceramic boat; 5, wool-like product (Moustache fibres); 6, $FeCl_2$ powder leftover; 7, black soot; 8, aluminium strings; 9, tungsten wedges; all scale bars, 1 cm; arrow indicates direction of acetylene flow for a, b and c images. (a) Reservoir locked before reaction. (b) Same after reaction (40 min), top view. Wool-like product was shaped by inner tube. (c) Same after removal of wool-like product. Ceramic boat was lifted from quartz plate of as much as 1 cm. (d) Diagram of reactor after reaction. External diameter: 3 cm.

3. Results and discussion

3.1. Production

After 40 min reaction, 800 mg of a grey fluffy wool-like product had emerged from the opening between ceramic boat and quartz plate, in such a volume that it occupied all space around ceramic boat (index 5 on Fig. 1). SEM observation of this product (Fig. 2a) showed mostly moustache-like carbon fibres, with some (typically 5% volume) disordered carbon nano-particles. These disordered carbon nano-particles were also found as the main compound of a black dense soot inside the ceramic boat (index 7 on Fig. 1d). Deep inside the ceramic boat, a small fraction of $FeCl_2$ powder was left intact (index 6 on Fig. 1d).

Acetylene to wool-like-product conversion rate was ~40 mass%. Production increased linearly with duration up to 40 min. $FeCl_2$ disappearance rate in reservoir was also linear (~5 mg/min).

The fibres (Fig. 2) were typically 10–100 μm long, 0.1–1 μm thick at centre, tapered to a few tens of nm at tips,

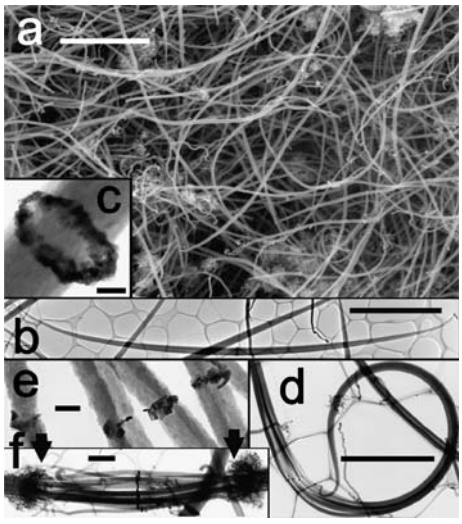

Fig. 2. Mid-magnification views of Moustache fibres (a, SEM; others, TEM). (a) Global view of the wool-like product. Scale bar 10 μm. (b) A mono-filament fibre. Scale bar 10 μm. (c) An iron-rich ring at centre of a mono-filament fibre. Scale bar 200 nm. (d) A multi-filament fibre with ~10 filaments. Scale bar 5 μm. (e) Iron-rich rings at centre of each filament of a multi-filament fibre. Scale bar 200 nm. (f) Centre of a multi-filament fibre including mistletoe-like balls (arrows) at junctions between mono and multi filament zones. Scale bar 1 μm.

with circular section. They had mirror symmetry at centre. In some cases, they consisted of only one filament (Fig. 2b, mono-filament type fibre). In other cases, they were divided in inner-filaments (up to several hundreds) at their centre, but not at extremities (Fig. 2d, multi-filament type fibres), somewhat reminding the morphology of a bundle of nanotubes. Fibre composition along body was determined by local SEM–EDX as carbon, with rare traces of Fe and Cl.

Remarkably, an iron-rich ring belted the centre of all (mono or multi) filaments (Fig. 2c,e). EDX analysis showed an elemental ratio Fe/Cl of 2/1 on the ring, indicating some remaining chlorine. Minor traces of oxygen were also observed. At very high resolution, rings appeared composed of metallic nano-crystals embedded in carbon (local electron diffraction on a ring gave polycrystalline pattern).

Typical fibre tip consisted of a tapered and poorly structured carbon filament with inner iron traces. A formation by erratic migration of a metal nano-particle is probable. Similar disordered filaments accumulation resembling mistletoe balls were sometime found at mono-filament fibre centre, or at junctions between mono and multi-filaments zones (arrows on Fig. 2f). An explosive formation is probable.

As-produced fibres were semi-crystalline, with a tendency to graphene layer alignment perpendicular to fibre axis, as shown by diffraction diagrams (Fig. 4a,c). However, fibres were readily crystallised by heat-treatment at 2800 °C. This resulted in a turbostratic lattice with layers nearly perpendicular to fibre axis, as observed by very high tension (800 kV) TEM on fibre sides (Fig. 3a) and diffraction patterns (Fig. 4b,d). The crystallisation was also attested by an improvement of burning resistance with heat-treatment (from 543 to 730 °C) in TGA; by a decrease of disorder/graphite (D/G) value with heat-treatment (from 1.03 to 0.28) in Raman analysis (Table 1). The relatively large interlayer distance indicated turbostratic piling, c-spacing having shrunk from 3.44 to 3.40 Å (Table 1). Other heat-treated carbon fibres produced by different CVD methods are known to show similar interlayer shrinking [10,14,15].

After heat-treatment, the turbostratic lattice (see electron diffraction of Fig. 4b) was not strictly perpendicular to fibre axis, but formed a wide-angle conical structure (at various angles, but 145° on Fig. 4b), fibre and cone axis being superposed, and cone pointing toward the tip of the fibre for each side of the fibre (TEM observation). This was clear after heat-treatment, but sometime also observable on raw fibres, as a tendency.

All metal contained in the product, including rings at fibre centres, were removed by heat-treatment (TGA left-over reduced from 5% to 0% mass with treatment).

As expected from near perpendicular layering, fibres were brittle. They were readily cleaved perpendicularly to axis by mortar crushing (this could enable the production of carbon micro-plates). Fibre centre was most easily broken. TEM observations showed poorest crystallinity in this zone.

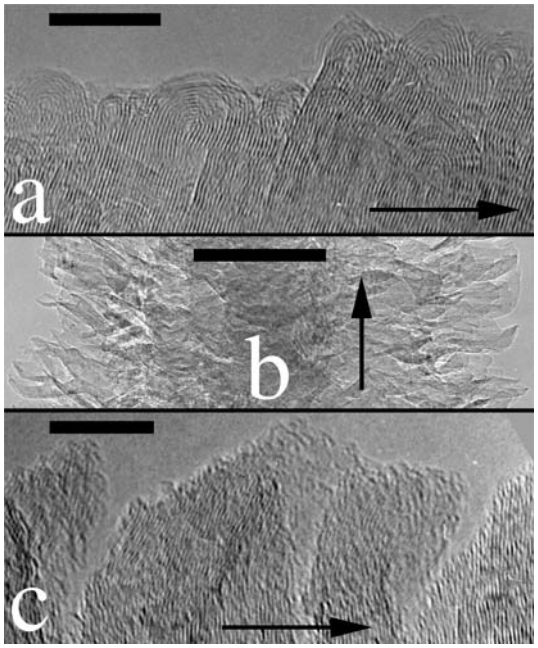

Fig. 3. 800 kV TEM views of thin Moustache fibres. Arrows indicate fibre axis and point toward fibre centre. (a) High-resolution view of a heat-treated fibre on outer surface. Graphene plane edges are not open-end, but bridged. Scale bar 10 nm. (b) Fibre after heat-treatment and 700 °C burning in air, slice view. Selective burning of graphene planes is observed. Scale bar 100 nm. (c) Enlargement of image b on fibre side. Bridging was removed. Scale bar 10 nm.

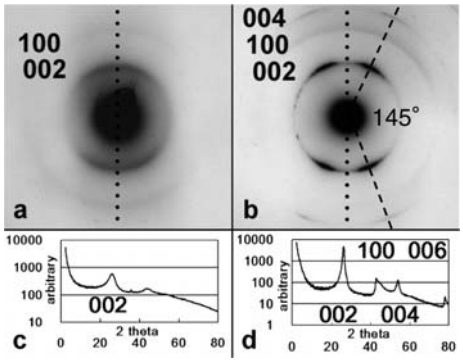

Fig. 4. Electron diffraction (a and b) for a thin filament (fibre axis on vertical dashed line), and powder X-ray diffraction (c and d) of wool-like product. (a) Raw Moustache fibre. A diffused 002 reflection is localised around fibre axis symmetrically. This indicates semi-crystalline structure, where graphene layers tend to align on fibre axis perpendicular. (b) Heat-treated Moustache fibre. 002 reflection is now well localised and separated in two, symmetrically to fibre axis. New 004 reflections have appeared. This corresponds to crystallisation in a conical structure with 145° angle, cone and fibre axis being superposed (additional TEM observations show that cones point toward fibre tips). (c) Powder X-ray of raw wool-like product. (d) Powder X-ray of heat-treated wool-like product.

After heat-treatment, graphene layer edges on fibre outer surface were observed bridged, and not open-ended (Fig. 3a), as usual with such treatment [16]. This bridging, which could be cumbersome for atomic absorption applications, was removed by air oxidation from 650 to 700 °C with weight loss of 20–70%. Oxidation resulted in a

Table 1
Macroscopic analyses of wool-like product before and after thermal treatment

	X-ray		TGA		Raman
	c (Å)	L_c (nm)	Burn T (°C)	Leftover (%)	D/G
Before	3.44	2.75	543	5 ± 3	1.03
After	3.40	12.8	730	0	0.28

X-ray data is extracted from Fig. 4c,d (Sherrer analysis method for X-ray 0 0 2 peak).

selective burning of graphene planes, and hence in a structure of high specific surface (Fig. 3b,c).

3.2. Discussion of growth mechanisms

It is clear from observations that fibres are produced outside reservoir, when inside reservoir only metal rich black soot is produced. This is probably because inside reservoir atmosphere is saturated with $FeCl_2$ vapours, and carbon input is limited. At 500 °C, vapour pressure of $FeCl_2$ is close to 10 Pa (exponential extrapolation from [17]). Traces of vapours, sometimes with recrystallisation, were observed around $FeCl_2$ powders.

Setting the optimum output $FeCl_2$ flow in between ceramic and quartz plate is critical for production. Experiments led at 475, 500, 525, and 550 °C gave a relative wool-like product mass of, respectively, 25%, 100%, 60%, 25%, showing a strong influence of temperature. (Furnace thermocouple temperature reading may be different from real reactor temperature due to radiative heating [18].)

In addition, mechanical stress in the reservoir caused by the accumulation of black soot, lifted the ceramic from quartz plate continuously during reaction (~0.2 mm/min), extending aluminium strings of as much as 1 cm (Fig. 1c). Experiments led with reservoir tightly locked gave no fibre product and little black soot, but left most $FeCl_2$ intact, because reservoir output was jammed.

On the other hand, the reservoir was necessary to inhibit direct reaction of carbon radicals with $FeCl_2$ powders. Experiments led with $FeCl_2$ powders open to carbon flow gave mostly black soot and very little Moustache fibres. (The reservoir probably also has a role in protecting $FeCl_2$ from residual oxidation during temperature setting.)

It is important to consider that $FeCl_2$ vapours are not decomposed at 500 °C, but directly react with carbon radicals from decomposed acetylene, to iron (cubic crystal), and chlorine (as chloro-carbons). This process is not fully understood at present, but likely leads to the formation of iron rings. The fact that solid $FeCl_2$ is highly 2D ($FeCl_2$ is a foiled hexagonal material [19]) may matter for formation of ring morphology.

Iron is a well known catalyst for the growth of carbon structures, helping the incorporation carbon atoms to growing atomic sites. When shaped as a ring, iron allows incoming carbon atoms to migrate to the inner walls of the ring, and nucleate pseudo graphene cones on each sides of the inner plane of the ring. This causes the growth of fibres from centre, and explains their specific structure of wide angle graphene cones pointing toward tips. The tapering of fibres indicates that rings progressively grow larger in diameter in the process.

Also, the fact that we observe multi-filaments and explosive formations, indicates that growth is highly unstable. Metals rings may violently divide to form, respectively, smaller rings (each catalysing a new growth), or spherical particles.

Acknowledgements

The author thanks M. Chokai, M. Kawamura, H. Kurimoto, Y. Matsui, S. Matsumura, H. Moriya, H. Sakurai, M. Sato, H. Suzuki, and C. Tsuruta for their help.

Appendix A. Supplementary data

Supplementary data associated with this article can be found, in the online version, at doi:10.1016/j.cplett.2006.11.091.

References

[1] A. Oberlin, M. Endo, J. Cryst. Growth 32 (1976) 335.
[2] K. Mukhopadhyay, A. Koshio, T. Sugai, N. Tanaka, H. Shinohara, Z. Konya, J.B. Nagy, Chem. Phys. Lett. 303 (1999) 117.
[3] C.N.R. Rao, A. Govindaraj, Acc. Chem. Res. 35 (12) (2002) 998.
[4] M.S. Kim, N.M. Rodriguez, R.T.K. Baker, J. Catal. 131 (1991) 60.
[5] M.S. Kim, N.M. Rodriguez, R.T.K. Baker, J. Catal. 134 (1992) 253.
[6] L.C. Qin, D. Zhou, A.R. Krauss, D.M. Gruen, Appl. Phys. Lett. 72 (26) (1998) 3437.
[7] V.I. Merkulov, D.H. Lowndes, Y.Y. Wei, G. Eres, E. Voelkl, Appl. Phys. Lett. 76 (24) (2000) 3555.
[8] H. Cui, O. Zhou, B.R. Stoner, J. Appl. Phys. 88 (10) (2000) 6072.
[9] M. Okai, T. Muneyoshi, T. Yaguchi, S. Sasaki, Appl. Phys. Lett. 77 (21) (2000) 3468.
[10] M. Endo et al., Appl. Phys. Lett. 80 (7) (2002) 1267.
[11] B.O. Boskovic, V. Stolojan, R.U.A. Khan, S. Haq, S.R.P. Silva, Nat. Mater. 1 (2003) 165.
[12] T. Laude, M. Chokai, H. Suzuki, S. Honda, H. Kuwahara, K. Sato, S. Matsumura, $FeCl_2$ as catalyst in nanotube CVD synthesis, in: Proceedings of the 27th Fullerene-Nanotubes General Symposium, Tokyo, 28–30 July 2004.
[13] T. Laude, Y. Matsui, Eur. Phys. J. Appl. Phys. 28 (2004) 293.
[14] J.S. Speck, M. Endo, M.S. Dresselhaus, J. Cryst. Growth 94 (1989) 834.
[15] L. Ci et al., J. Cryst. Growth 233 (2001) 823.
[16] M. Endo et al., Carbon 41 (2003) 1941.
[17] D.R. Lide (Ed.), CRC Handbook of Chemistry and Physics, 73rd ed., CRC press, Boca Raton, 1992–1993.
[18] T. Laude, Y. Matsui, Eur. Phys. J. Appl. Phys. 28 (2004) 173.
[19] R. Colton, J.H. Canterford, Halides of the Transition Elements I – Halides of the First Row Transition Metals, Wiley-interscience, John Wiley & Sons Ltd., London, 1969.